VECTOR MAGNETIC FIELDS IN PROMINENCES: Observations and Analysis

R.N. Smartt
National Solar Observatory
National Optical Astronomy Observatories[*]
Sunspot, NM 88349, U.S.A.

and

L.L. House
High Altitude Observatory
National Centre for Atmospheric Research[**]
Boulder, CO 80307, U.S.A.

Abstract

Measurements of the polarization of the He I D_3 multiplet in a prominence allow the magnetic fields associated with the prominence to be deduced. The amount and angle of the linear polarization are governed by the Hanle effect, the detailed theory of which is applied to the Stokes components of the He I D_3 emission to derive the associated vector magnetic fields. The dependence of the observed polarization on the magnetic field is predicted from solutions of the statistical equilibrium equations for the He I D_3 multiplet. Magnetic field vector solutions for each pair of linear polarization Stokes profiles corresponding to an observational point in a prominence are not uniquely determined. Nevertheless, physically correct solutions can usually be identified with a high confidence level. Field vectors are mostly close to horizontal and normal to the prominence surface, magnitudes ranging from 6 G to 60 G, with a mean of 24 G.

1. Introduction

The key to understanding the structure and origin of prominences lies in establishing their vector magnetic field configuration. Zeeman-effect magnetograph measurements allow only the longitudinal (line-of-sight) component of the field to be measured with reasonable accuracy (±1 G) and with a moderate sensitivity down to ~1 G, while measurements of the transverse component have an estimated sensitivity of only 50 G (Leroy, 1979), a value apparently much larger than typical field strengths within quiescent prominences. Moreover, it is now generally recognized that the validity of such measurements and the accuracy of the corresponding derived fields, interpreted by the Zeeman effect can be severely limited by resonance polarization contributions. In the case of He I D_3, for example, the observed circular polarization results both from the Zeeman effect and from level crossing interference in the Hanle effect (Landi Degl' Innocenti, 1982). Also, radiative transfer effects in commonly used lines such as H_α substantially complicate the magnetic field interpretation.

Polarization due to resonance scattering, modified by the presence of a magnetic field- the Hanle effect - is a sensitive and accurate indicator of the vector magnetic field in a prominence. The Hanle effect occurs in a weak magnetic field when the Zeeman splitting is comparable to the natural width of the component sublevels; the resulting partial degeneracy of the level mixes the polarization properties of the Zeeman sub-levels. This mixing partially depolarizes radiation and reorients the plane of polarization of radiation undergoing resonance scattering. The extent of the depolarization depends upon the magnitude and direction of the field. From the amount of the depolarization and rotation, one may deduce the vector magnetic field associated with a prominence.
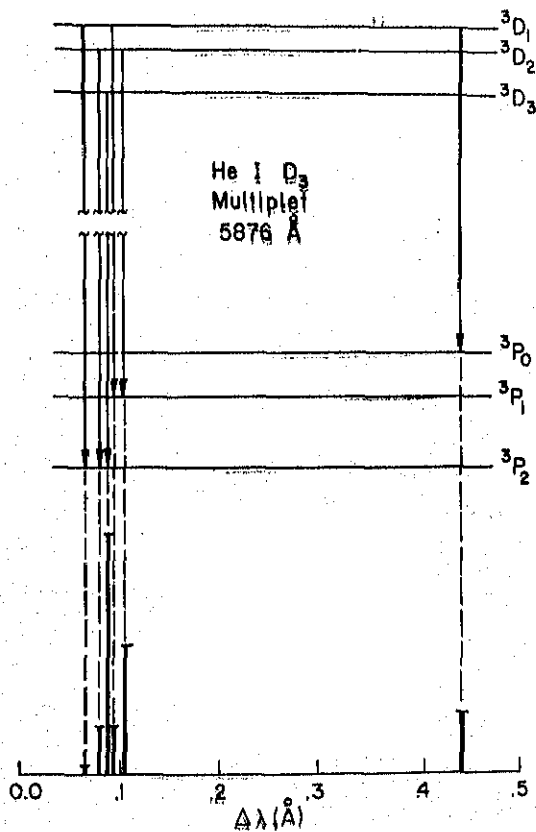
The D_3 (5876 Å) spectral profile has two well-defined components. The major (blue) component results from five transitions, $3^3D_3-2^3P_2$, $3^3D_2-2^3P_2$, $3^3D_2-2^3P_1$, $3^3D_1-2^3P_2$ and $3^3D_1-2^3P_1$, while the minor (red) component is a simple triplet, $3^3D_1-2^3P_0$, producing an extended wing in the profile. The peaks are separated by about 0.34 Å. The relative magnitudes and spectral locations of the D_3 transitions are shown in Figure 1. The two components of the profile have different polarization sensitivities to magnetic field strengths (House and Smartt, 1979, 1982), and if spectrally resolved and isolated by Gaussian curve fitting, two independent measurements of linear polarization (from the Q and U Stokes scans) are obtained. A histogram of linear polarization values, P(1), associated with the major component of the profile, representing 83 measurements of quiescent prominences, is shown in Figure 2a. Figure
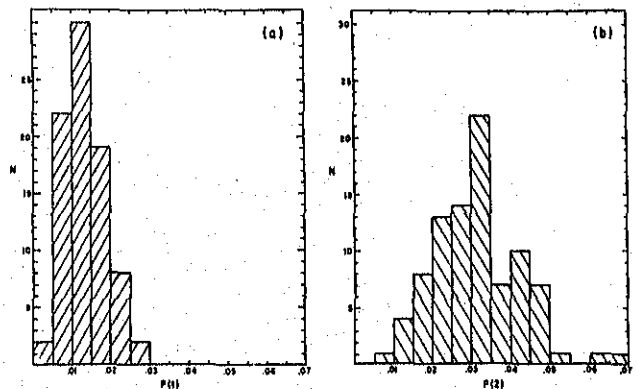

Fig.1.   The relative magnitudes and spectral locations of the transitions that form the He I D$_3$ multiplet.

Fig.2.   Histograms of the linear polarization, P, as observed in quiescent prominences corresponding to a) the major component of the D$_3$ profile (P(1)), and b) the minor component of the D$_3$ profile (P(2)).

2b is a corresponding histogram of the polarization, P(2), of the minor component revealing the significantly different distribution of P(1) and P(2). This difference in sensitivity produces some redundancy (for

perfect data) in the information required to deduce the vector field. Further, Landi Degl' Innocenti (1982) has completed the theory of D_3 by computing the expected circular polarization profile for a given configuration of the magnetic field vector. The observed circular polarization V profiles can then be interpreted. Since the resultant data from the V profiles are independent, ambiguities intrinsic to interpreting polarimetric data of prominences in D_3 can be resolved. However, observationally the V component is frequently noise-dominated and hence uninterpretable. Additional advantages of D_3 are that it is both optically thin and relatively bright in prominences. Most importantly however, the statistical equilibrium equations have been solved in sufficient detail (Bommier et al. 1981; Landi Degl' Innocenti, 1982) that D_3 may be interpreted with confidence. Here we report on measurements of vector magnetic fields associated with a quiescent prominence, obtained by interpeting spectrally resolved Stokes scans of D_3. For a more detailed description of this work, refer to House and Smartt (1982), Athay et al. (1983) and Querfeld et al. (1984).

2. Observations

The D_3 polarimetric observations of the prominence discussed here were obtained on April 19-22, 1978, using the HAO/SPO Stokes-I polarimeter (Baur et al. 1980). A set of Stokes profiles, coresponding to one observational point (3.5 arc sec x 10 arc sec), represents 100 spectral scans recorded in about 20 minutes. The dispersion of the prominence in both H_α and D_3 on four consecutive days of observations, as well as on April 23, is shown in the spectroheliograph images of Figure 3 (at approximately 14:00 UT). Note the significant evolution of the prominence over a four-day period. This prominence occurred in the S-E, extending in longitude over
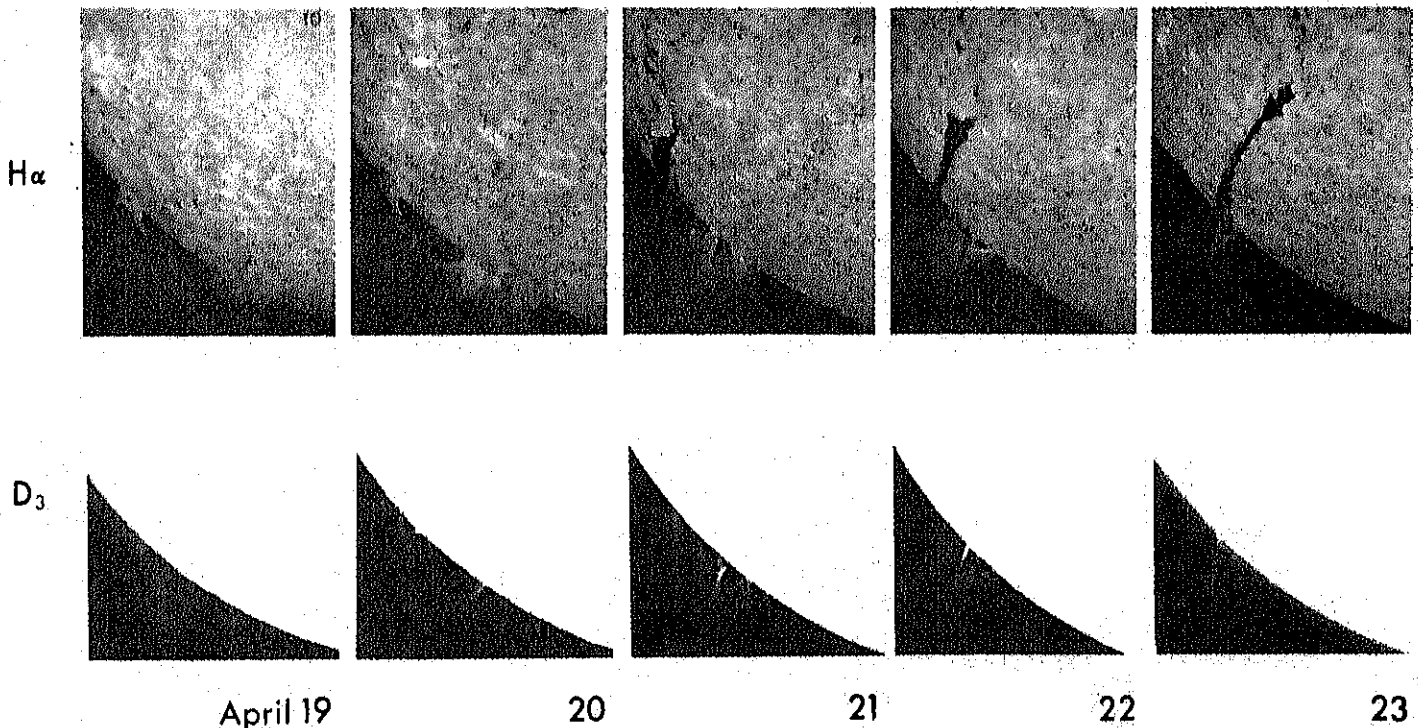

Fig.3. Spectroheliograph images in H_α and D_3 of a large quiescent prominence of which polarimetric observations were obtained, April 19-22, 1978. Approximately one hour after the last image was recorded, the prominence erupted.

about 75°, and in latitude from approximately 31° to 52°. The long axis of the prominence was inclined by about 30° to the line of sight. The maximum height was ~ 10^5 km. This prominence erupted abruptly soon after 14:00 UT on April 23.

A sample of a typical set of four D_3 Stokes spectral profiles, intensity, I, linear polarization, Q and U, and circular polarization, V, is shown in Figure 4. The ordinate
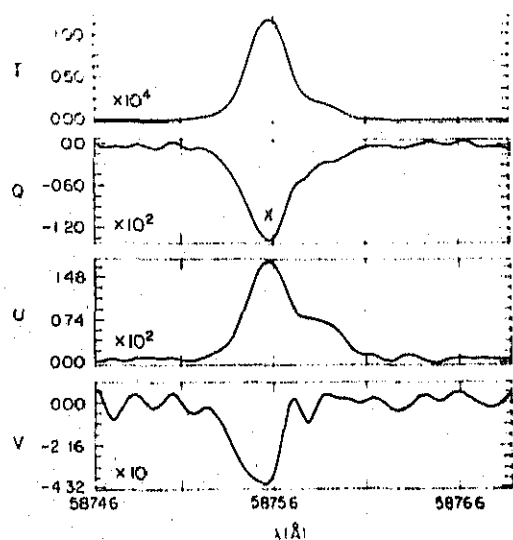

Fig. 4. A typical set of Stokes profiles in D_3. units are millionths of the central disk spectral brightness. The linear polarization degree (of the major component) is about 2% while the circular polarization is a factor of four smaller. Instrumental noise levels were below 10^{-3} in polarization. Note that a two-slit magnetograph measurement of V would be very misleading.

3. Data Processing

Polarimetric observations such as those shown in Figure 4 are initially smoothed and fitted with Gaussians to obtain the relevant polarization parameters. As well, they must be augmented with supplementary information

necessary for their interpretation.

The polarization reference axis assumed in both the Bommier (1981) and Landi Degl' Innocenti (1982) statistical equilibrium solutions lies along the local radius so that Q and U must be rotated from the instrument coordinates, E-W geocentric, into the radial reference frame. In addition, the apparent height, h, of the observation above the limb and the dihedral angle, χ, between the plane of the sky and the heliocentric radius through the observed point are necessary. h and χ together give the true height, $r = (R_0 + h) \cos \chi$. The angle χ is also needed to determine the disk-prominence-observer scattering angle. The measurement of χ is invariably uncertain. It is best obtained by tracking a specific point on the prominence over a period of time. Such a sequence of observations, ideally over several days, even if available, has limited precision due to the general evolution in form of all prominences even on a time scale of a few hours.

All of the amplitudes for I, Q, U and V are normalized to the intensity to obtain blue and red values of Q/I, U/I, and V/I, proportional to the integrated strengths of the multiplet components. This results in four linear polarization values $(Q/I)_{red}$, $(Q/I)_{blue}$, $(U/I)_{red}$, $(U/I)_{blue}$, which are used to obtain plausible, but usually ambiguous values for field strengths, $|\underline{B}|$, and direction (θ, ϕ), where θ is the field polar angle measured from the local radius and ϕ is the azimuthal angle measured around the local radius, with $\phi = 0°$ pointing west and $\phi = 90°$ pointing north. The remaining data, $(V/I)_{blue}$ and $(V'/I)_{blue}$ (where V' is the derivative of V) are used to reduce the ambiguities inherent in the Q, U interpretation.

3.1. Hanle Effect Codes for He I D$_3$

Bommier et al. (1981) and Landi Degl' Innocenti (1982) have independently constructed Hanle effect codes for the magnetic field interpretation of prominence Stokes profiles in He I D$_3$.

From the Stokes profiles, the observational parameters of intensity and the corresponding two-dimensional linear polarization vectors for both the blue and red components of the D$_3$ multiplet, as well as values for h and χ , are employed in the interpretation.

Essentially two sets of equations must be solved. The first relates the density-matrix components of the atomic system to the properties of the incident radiation field and the second describes the properties of the emitted radiation in terms of the density matrix. An inversion procedure, incorporating a transformation from the coordinate system used conventionally in the theory to that of the instrument, is then used to determine corresponding magnetic field values. The Bommier code simplifies the computational procedure by calculating the field for a height of 50 arc sec and scaling this value for any given observational height, whereas the Landi Degl' Innocenti code computes β in increments of 10 arc sec in height, and interpolates between heights. The Landi Degl' Innocenti code also incorporates an interpretation of Stokes V-profile data, which consists of an independent intensity-like component, $\phi(\lambda)$, and a Zeeman component, $\delta\phi/\delta\lambda$ (Landi Degl' Innocenti, 1982). This interpretation proves to be cruical in sifting out a single value for the magnetic field from a typical set of solutions, as discussed in Section 4 below. Since the Bommier code was available in a fully-developed form, it was used almost exclusively for the results reported here.

4. Results

4.1. Multiple Solution and Sifting Procedures

It has been verified that synthetic linear polarization data, used as input, result in unique magnetic field vector solution, or at most a symmetrical pair of solutions. The ambiguity is intrinsic to scattering polarization in the presence of a magnetic field (see Landi Degl' Innocenti, 1982). However, when observational data are used multiple-valued solutions are generally produced that satisfy the fundamental requirement that a vector magnetic field predicted by one component of the D$_3$ profile is also predicted by the other. The inversion procedure of the code searches for the best solutions based on this criterion, in terms of a so-called distance function, D, where

$$D = \sqrt{\sum_i [(\Delta Q_i)^2 + (\Delta U_i)^2]}$$

and where Q_i = $(Q_i theo - Q_i obs)/I$, the summation index running on the two components of D$_3$ line. The lack of uniqueness apparently result from residual noise, spatial and temporal averaging and imprecision in the geometrical parameters, all inherent in the observational data.

Various procedures have been used to sift out invalid solutions. The most straight forward is where the V-profile is well defined. Theoretical V-profiles can be constructed from the linear polarization solutions and compared with the observed profiles. This procedure can be sufficient to isolate the correct solution. As pointed out in the previous section, the V-profile consists of a component proportional to intensity and a Zeeman component, proportional to the derivative of the intensity, the two components denoted here by V and V', respectively. The presence of V' therefore is evidence of a longitudinal component of the field

and its absence that the field is very nearly transverse. Further, the signs of Q, U, V and V' can be compared for self-consistency for a given set of B, h and χ, and many solutions rejected on this basis. As an extension of this procedure, polarization maps for Q, U, V and V', for both components, so-called altitude diagrams, have been prepared. These are contour maps of polarization on a θ, φ plane for a given B, h, χ set. By intercomparing a set of corresponding maps, inadmissible solutions can be readily identified.

By such methods, it is frequently found that all tentative solutions can be eliminated except a symmetrical pair. The correct direction can then be identified, at least with modest confidence, by comparison with photospheric magnetic fields. Uncertainty arises primarily from the possible substantial evolution of a field distribution between the time of the prominence observations and that of the magnetograph record. Finally, self-consistency provides a further, general check on the validity of a set of solutions representing measurements in the same prominence, especially if such measurements are repeated on two or more days.

4.2. Summary of Magnetic Field Solutions

The prominence measurements discussed here constitute a particularly useful set in that the profiles are generally of good quality (36 of 44 of the observed points are interpretable in the linear polarization) and extend over four consecutive days, during which time the prominence gradually evolved in form and systematically increased in height. Since this prominence was relatively high and extensive and was observed over a four-day period, estimates of h and χ could be obtained with more confidence than for typical prominences.

The complete set of magnetic field vector solutions are presented in Figure 5. The dashed outline of the prominence,
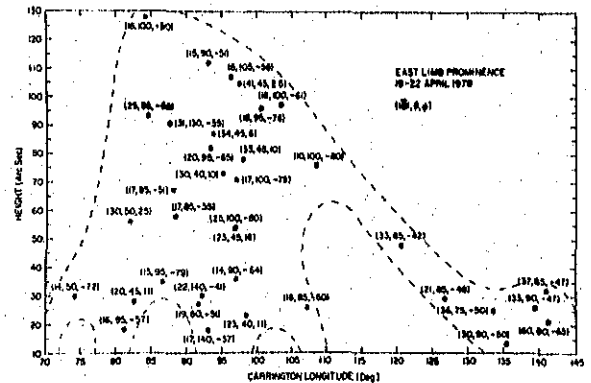
Fig.5.   Vector field orientations and positions in the 19-22 April, 1978 quiescent prominence. The number sets are field strength, B (gauss), the polar angle, θ (degrees), measured from the local radius, and the azimuthal angle, φ(degrees), around the local radius. Zero azimuth points west, +90° points north.

imprecise because of the changing form of the prominence over the four-day period, is intended to give simply a general frame of reference. Note the tendency for large values of $|\underline{B}|$ to occur in the leg of the prominence and that most of the remaining above-average values occur in the central part of the bulk of the prominence. The mean value is 23.8 G.

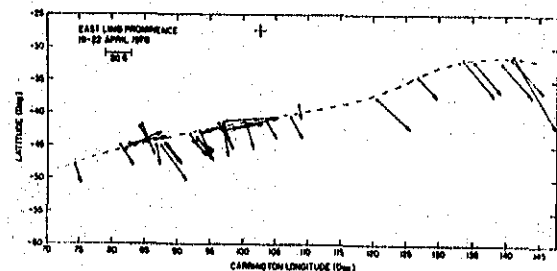Figure 6 is a latitude-longitude plot of field vectors for the same data set of

Fig.6.   Latitude-longitude plot of field vectors for the 19-22 April, 1978 prominence. Arrows are proportional to the field strength. Surface magnetograph polarities are shown.

Figure 5. The length of the arrows are proportional to the field strength. The dashed line represents an approximate outline of the prominence as seen as a filament. The plus and minus signs indicate the surface magnetograph polarities. With some marked exceptions, the tendency for the horizontal component of the field vector to lie close to 90° from the long axis of the prominence is obvious.

5. Comments

It has been pointed out above that the polarimeter field aperture, 3.5 arc sec by 10 arc sec, is large compared to the fine threads of emitting material, ~1 arc sec or smaller, that are sometimes observed in high resolution images of prominences. If such threads represent corresponding fine-scale magnetic structure, rather than simply being evidence of thermal instabilities, the observed mean polarization would be larger than that representative of the magnetic elements and the magnitude of the deduced magnetic field values would be correspondingly reduced. Implicit in the procedure for magnetic field derivation then is the assumption that the magnetic field is homogeneous over the polarimeter angular aperture. But even if the magnetic field is uniform over the field sampled by the polarimeter, line of sight contributions are likely to have a mixture of field components, which would result in a diminution of observed polarization and an increase to an unknown degree of inferred field strengths. The further assumption that the prominence material is effectively stationary during the period of observation is also not necessarily valid, and if so, the effect is also to increase the inferred field strengths.

Conclusion

Stokes polarimeter spectral profiles of He I D_3, representing many observational points within a quiescent prominence, have been interpreted using a detailed quantum-mechanical theory of resonance polarization for the D_3 multiplet. The multiple set of solutions obtained when the linear polarization information alone is used can be reduced, generally to a symmetric pair, when the full, generalized theory is applied that interprets also the weak circular polarization Stokes profile. In most cases a unique solution can be found through additional information available from disk field polarity.

Most of the derived magnetic field vectors are close to horizontal and near normal to the prominence surface, with some extreme exceptions, thus generally supporting the Kippenhahn-Schluter (1957) model. The values obtained for the magnetic field vectors are thought to be mostly accurate representations of the actual prominence fields, a mean for this prominence of 24 G.

References

Athay, R.C., Querfeld, C.W., Smartt, R.N., Degl' Innocenti, E.L., and Bommier, V., 1983, Solar Phys. 89, 3.

Baur, T.G., House, L.L., and Hull, H.K., 1980, Solar Phys. 65, 111.

Bommier, V., Leroy, J.L., and Sahal-Brechot, S., 1981, Astron. Astrophys. 100, 231.

House, L.L., and Smartt, R.N., 1979, In E. Jensen et al. (eds), "Physics of Solar Prominences", Institute of Theoretical Astrophysics, Oslo, p.81.

House, L.L., and Smartt, R.N., 1982, Solar Phys. 80, 53.

Kippenhahn, R., and Schluter, A., 1957, Z. Astrophys. 43, 36.

Landi Degl' Innocenti, E., 1982, Solar Phys. 79, 291.

Leroy, J.L., 1979, in E.Jensen et al. (eds), "Physics of Solar Prominences", Institute of Theoretical Astrophysics, Oslo, p.56.

Querfeld, C.W., Smartt, R.N., Bommier, V., Landi Degl' Innocenti, E., and House, L.L., 1984, (Submitted to Solar Phys.)

DISCUSSION:

BHATTACHARYYA: (1) How do you calculate the strength of the magnetic field? Are there any calibrations from laboratory measurements?

SMARTT: (1) The strength of the magnetic field is calculated by applying the theory of the Hanle effect for He I D_3 line to the observed polarization. There has been no laboratory verification.

BHATTACHARYYA: (2) Cannot one measure the field in prominences by Zeeman method?

SMARTT: (2) Earlier attempts to measure magnetic field strengths in prominences based on the Zeeman effect, one now recognized as being invalid due to the dominence of the Hanle effect in the magnetic field regime appropriate for prominences, and especially so for lines which are not optically thin in prominences.

VINOD KRISHAN: Have there been any attempts to produce analytic functional forms of the magnetic field from the derived numbers?

SMARTT: So far, we have obtained only the vector magnetic field functions. We plan to investigate statistical relationships of the cumulative data and especially to use this information to try to understand the observed morphology of quiescent prominences.